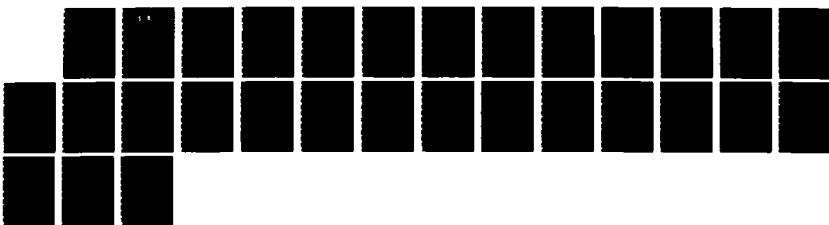
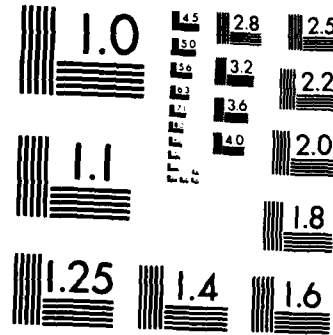


AD-A172 984    BASIC INSTABILITY MECHANISMS IN CHEMICALLY REACTING  
SUBSONIC AND SUPERSONIC FLOWS(U) MASSACHUSETTS INST OF  
TECH CAMBRIDGE T TOONG 21 OCT 85 AFOSR-TR-86-0887    1/1  
UNCLASSIFIED AFOSR-83-0373    F/G 21/2    NL





MICROCOPY RESOLUTION TEST CHART  
NATIONAL BUREAU OF STANDARDS-1963-A

UNCLASSIFIED

AD-A172 904

SECURITY CLASSIFICATION OF THIS PAGE

(2)

## REPORT DOCUMENTATION PAGE

1a. REPORT SECURITY CLASSIFICATION UNCLASSIFIED		1b. RESTRICTIVE MARKINGS None										
2a. SECURITY CLASSIFICATION AUTHORITY SELECTE		3. DISTRIBUTION/AVAILABILITY OF REPORT Approved for public release, Distribution unlimited										
2b. DECLASSIFICATION/DOWNGRADING SCHEDULE Sect 08 1986		4. PERFORMING ORGANIZATION REPORT NUMBER(S) D										
6a. NAME OF PERFORMING ORGANIZATION Massachusetts Inst. of Tech.		6b. OFFICE SYMBOL (If applicable)										
6c. ADDRESS (City, State and ZIP Code) Cambridge, MA 02139		7a. NAME OF MONITORING ORGANIZATION Air Force Office of Scientific Research										
8a. NAME OF FUNDING/SPONSORING ORGANIZATION Air Force Office of Scientific Research		8b. OFFICE SYMBOL (If applicable) AFOSR/NA										
8c. ADDRESS (City, State and ZIP Code) Bolling AFB, D.C. 20332-6448		9. PROCUREMENT INSTRUMENT IDENTIFICATION NUMBER AFOSR-83-0373										
11. TITLE (Include Security Classification) Basic Instability Mechanisms in Chemically Reacting Subsonic and Supersonic Flows		10. SOURCE OF FUNDING NOS.  PROGRAM ELEMENT NO. 61102F      PROJECT NO. 2308      TASK NO. A2      WORK UNIT NO.										
12. PERSONAL AUTHOR(S) Tau-Yi Toong												
13a. TYPE OF REPORT Annual		13b. TIME COVERED FROM 30/9/84 TO 29/9/85										
14. DATE OF REPORT (Yr., Mo., Day) 1985, October, 21		15. PAGE COUNT 28										
16. SUPPLEMENTARY NOTATION												
17. COSATI CODES <table border="1"><tr><th>FIELD</th><th>GROUP</th><th>SUB. GR.</th></tr><tr><td>21</td><td>01</td><td></td></tr><tr><td>21</td><td>02</td><td></td></tr></table>		FIELD	GROUP	SUB. GR.	21	01		21	02		18. SUBJECT TERMS (Continue on reverse if necessary and identify by block number) Turbulence-Combustion Interactions Instability Mechanisms Disturbed and Turbulent Flames	
FIELD	GROUP	SUB. GR.										
21	01											
21	02											
19. ABSTRACT (Continue on reverse if necessary and identify by block number) Both theoretical and experimental studies were conducted to determine and elucidate major mechanisms governing turbulence-combustion interactions. The theoretical study showed the importance of "wrinkling-like" effects as well as the effects of the chemical reaction rate on the evolution of fluctuations in streamwise- and transverse-velocity, temperature, concentration, and vorticity in a shear layer. The "wrinkling-like" effects were induced by the transverse-velocity fluctuations in nonuniform mean flows. The direct rate-augmentation effects due to reaction led to changes in phase relationships between the various fluctuations, resulting in turbulent energy and mass transport in a direction opposite to that suggested by the gradient model in that part of the shear layer nearer the unreacted region. The experimental study showed the effects of adding ethane (at the same overall equivalence ratio) on the thermal structure of methane/air flames. Temperature fluctuations were augmented by ethane addition, the highest augmentation being observed at 10%-ethane addition. A one-component Laser-Doppler-Velocimetry system was installed and tested. A manuscript on the genesis of transverse waves in gaseous detonations was accepted for publication in												
20. DISTRIBUTION/AVAILABILITY OF ABSTRACT UNCLASSIFIED/UNLIMITED <input checked="" type="checkbox"/> SAME AS RPT. <input type="checkbox"/> DTIC USERS <input type="checkbox"/>		21. ABSTRACT SECURITY CLASSIFICATION UNCLASSIFIED										
22a. NAME OF RESPONSIBLE INDIVIDUAL Dr. Julian M. Tishkoff		22b. TELEPHONE NUMBER (Include Area Code) (202) 767-4935										
22c. OFFICE SYMBOL AFOSR/NA		DTIC FILE COPY										

**UNCLASSIFIED**

SECURITY CLASSIFICATION OF THIS PAGE

Combustion and Flame. A manuscript on turbulence-combustion interactions was in preparation.

Accesion For	
NTIS CRA&I	<input checked="" type="checkbox"/>
DTIC TAB	<input type="checkbox"/>
Unannounced	<input type="checkbox"/>
Justification .....	
By .....	
Distribution /	
Availability Codes	
Dist	Avail and/or Special
A-1	



**UNCLASSIFIED**

SECURITY CLASSIFICATION OF THIS PAGE

**AFOSR-TR- 86-0887**

Approved for public release;  
distribution unlimited.

AIR FORCE OFFICE OF SCIENTIFIC RESEARCH (AFSC)  
NOTICE OF TRANSMISSION TO DTIC  
This technical report has been reviewed and is  
approved for public release IAW AFR 190-12.  
Distribution is unlimited.

MATTHEW J. KEMPER  
Chief, Technical Information Division

ANNUAL TECHNICAL REPORT ON RESEARCH  
SUPPORTED BY GRANT AFOSR-83-0373  
(September 30, 1984-September 29, 1985)

Basic Instability Mechanisms  
in Chemically Reacting Subsonic and Supersonic Flows  
Tau-Yi Toong  
Massachusetts Institute of Technology

Summary of Progress

Both theoretical and experimental studies were conducted to determine and elucidate major mechanisms governing turbulence-combustion interactions. The theoretical study showed the importance of "wrinkling-like" effects as well as the effects of the chemical reaction rate on the evolution of fluctuations in streamwise- and transverse-velocity, temperature, concentration, and vorticity in a shear layer. The "wrinkling-like" effects were induced by the transverse-velocity fluctuations in nonuniform mean flows. The direct rate-augmentation effects due to reaction led to changes in phase relationships between the various fluctuations, resulting in turbulent energy and mass transport in a direction opposite to that suggested by the gradient model in that part of the shear layer nearer the unreacted region. The experimental study showed the effects of adding ethane (at the same overall equivalence ratio) on the thermal structure of methane/air flames. Temperature fluctuations were augmented by ethane addition, the highest augmentation being observed at 10%-ethane addition.

A one-component Laser-Doppler-Velocimetry system was installed and

tested. A manuscript on the genesis of transverse waves in gaseous detonations was accepted for publication in Combustion and Flame. A manuscript on turbulence-combustion interactions was in preparation.

## I. Objectives and Scope of Work

The main objectives of this research are to determine and elucidate major mechanisms governing turbulence-combustion interactions in different spectral regimes and to provide sound basis for formulating guidelines for improving combustion efficiency and reducing emissions. During the past year, both theoretical and experimental studies were conducted. The theoretical study showed the importance of "wrinkling-like" effects as well as the effects of the chemical reaction rate on the evolution of various fluctuations, and the experimental study showed the effects of adding various amounts of ethane (at the same overall equivalence ratio) on the thermal structure of methane/air flames. Both studies demonstrated the important roles of chemical kinetics in augmenting the temperature fluctuations within turbulent flames.

A one-component Laser-Doppler-Velocimetry (LDV) system was installed and tested. A manuscript on the genesis of transverse waves in gaseous detonations was accepted for publication in Combustion and Flame. A manuscript on turbulence-combustion interactions was in preparation.

## II. Results and Discussion

### (1) Turbulence-Combustion Interactions

#### (A) Theory

In order to understand the origin, nature, and governing mechanisms in turbulence-combustion interactions, the stability of a chemically

reacting shear layer with streamwise-velocity, concentration, and temperature gradients in the transverse direction under the influence of a longitudinal (or streamwise) pressure disturbance was examined. Figure 1 shows the flow field in a shear layer of thickness  $2\delta$ . The pressure disturbance was assumed to be a travelling wave with its initial amplitude  $\pi_0$  at  $y = -\delta$ , next to the unreacted region. Chemical reaction occurred in the region between  $y = -\delta$  and  $+\delta$ . In this two-dimensional model it was expected that the interactions between the pressure and the density or entropy fluctuations would lead to the generation of vorticity, which is one of the three basic modes of fluctuations in turbulence.

The governing equations showed the following:

- (a) The propagation of the pressure disturbance was affected by the presence of the mean transverse streamwise-velocity and temperature gradients as well as the fluctuations in the chemical reaction rate.
- (b) The streamwise-velocity fluctuations were affected mainly by the mean transverse velocity gradient while the temperature, concentration, and vorticity fluctuations were affected mainly by the corresponding mean transverse gradient and the fluctuations in the chemical reaction rate. The effects of pressure fluctuations were comparatively small at low Mach numbers and for relatively long wavelength of the pressure disturbance with respect to the shear-layer thickness.
- (c) The transverse velocity fluctuations were induced by the non-uniform distribution of the pressure fluctuations in the transverse direction.
- (d) Fluctuations in the streamwise-velocity, concentration, temperature, and vorticity were induced through a "wrinkling-like" effect

due to the coupling between the transverse velocity fluctuations and the corresponding mean transverse gradients.

(e) In addition to the "wrinkling-like" effect, there was the direct rate-augmentation effect on the concentration, temperature, and vorticity fluctuations due to chemical reaction.

(f) The direct chemical effects were found to depend on the activation energy, order, and enthalpy of reaction as well as Damköhler's first and third parameters.

Numerical solutions of the governing equations for the case of small shear-layer thickness relative to the wavelength of the pressure disturbance showed that the flow was always unstable, leading to amplification of all fluctuations. Figure 2 shows the effects of chemical reaction on the growth rate ( $-\alpha c_i$ ) versus the wave number ( $\alpha$ ) or the inverse wavelength. The case of a nonreacting shear layer with no transverse temperature gradient was found to be the most unstable. In the presence of the transverse temperature gradient, with or without chemical reaction, the flow became less unstable. Nevertheless, the flow was more unstable with chemical reaction, with increasing amplification rate for higher activation energy and faster chemical reaction rate. Also, with increasing wave number or decreasing wavelength of the pressure disturbance, the amplification rate per second increased while the amplification rate per cycle decreased.

In order to elucidate the coupling mechanism governing turbulence-combustion interactions, the phase relationships between the various fluctuations were examined. Figures 3-6 show the complex eigenfunctions representing the fluctuations in the phase plane at different positions  $\eta$

within the shear layer with and without chemical reaction. Figure 3 shows a comparison of the pressure fluctuations  $\hat{p}/\pi_0$  for three cases: case 1, no reaction and no transverse temperature gradient; case 2, no reaction but with transverse temperature gradient; and case 4, with reaction and transverse temperature gradient. No significant differences in the amplitudes and the phase angles were observed.

Figure 4 shows comparisons of the velocity fluctuations in the streamwise direction  $\hat{u}/\pi_0$  and the transverse direction  $\hat{v}/\pi_0$  with and without reaction (case 4, on the left, and case 2, respectively). Large changes in the amplitudes and the phase angles were observed at different positions within the shear layer. (Note that the amplitudes were in logarithmic scale.) The difference between reacting and nonreacting case, however, was small.

Figure 5 shows a comparison of the complex eigenfunctions for the temperature fluctuations  $\hat{T}/\pi_0$ . For case 2, with no chemical reaction,  $\hat{T}/\pi_0$  remained in the first quadrant with rather small change in the phase angles at different positions. On the other hand, for case 4 with chemical reaction, the phase angles changed rather drastically within the shear layer from  $\eta = 0.01$  (near the unreacted region) to  $\eta = 0.98$  (near the completely reacted region). Thus, the main effect of chemical reaction is to cause large changes in the phase angles, leading to rather complex coupling between different fluctuations.

A comparison of the vorticity fluctuations  $\hat{\Omega}/\pi_0$  was shown in Fig. 6. With no reaction (case 2), the vorticity eigenfunction varied between the first and the third quadrant almost along a straight line. However, with reaction (case 4), rather complex changes in the phase angles were observed

at different positions within the shear layer with accompanying large changes in the amplitudes, thus signifying substantial effects on the turbulent structure.

The physics of the coupling between different fluctuations was further elucidated in Figs. 7-10. Figures 7 and 8 show the phase relationships between the temperature and the transverse-velocity fluctuations at two positions within the shear layer, one near the unreacted region ( $\eta = 0.2$ ) and the other near the completely reacted region ( $\eta = 0.8$ ). The expressions on the top of these figures showed their relationships. As noted earlier from the governing equations, the temperature fluctuations were induced through a "wrinkling-like" effect due to the coupling between the transverse velocity fluctuations  $\hat{V}/\pi_0$  and the mean transverse temperature gradient  $dT^*/d\eta$  (cf. the right-hand side of the expression at the top of Figs. 7 and 8) and through direct rate-augmentation effect due to chemical reaction (cf. second term on the left-hand side of the expression, where  $D_I$  and  $D_{II}$  were Damköhler's first and second parameters, respectively, and  $\beta$  and  $m$  were the nondimensional activation energy and the order of the assumed Arrhenius rate expression, respectively).

One important point to be noted in Figs. 7 and 8 was the relative phase difference at  $\eta = 0.2$  and  $0.8$  with and without chemical reaction. Without chemical reaction, the angle between  $\hat{T}$  and  $\hat{V}$  was obtuse at both positions, while with chemical reaction, the angle was obtuse at  $\eta = 0.8$  but acute at  $\eta = 0.2$ , thus accounting for the change in the direction of the turbulent energy transport with respect to the mean temperature gradient (to be discussed later in connection with Fig. 11a).

The phase relationships between the vorticity, temperature, and

transverse-velocity fluctuations were shown in Figs. 9 and 10 for two positions within the shear layer. Again, the expressions at the top showed the wrinkling-like effect and the direct rate-augmentation effect on vorticity fluctuations (cf. the first and the second term on the right-hand side of the expression, respectively). Note that the chemical effect appeared through temperature fluctuations. With or without chemical reaction, the angle included between  $\hat{\omega}$  and  $\hat{v}$  remained obtuse at  $\eta = 0.2$  and became acute at  $\eta = 0.8$ .

Normalized cross-correlation of the temperature and the transverse-velocity fluctuations with and without chemical reaction was shown in Fig. 11a. For non-reacting flows (case 2), the correlation remained negative within the entire shear layer, indicating that the turbulent energy transport could be related to the mean transverse temperature gradient on the basis of an "eddy-diffusivity" model. On the other hand, with chemical reaction (case 4), the correlation was positive in that part of the shear layer nearer the unreacted region, indicating the inappropriateness of the gradient model to account for the turbulent energy transport.

Similar behavior was observed for the normalized cross-correlation of the concentration and the transverse-velocity fluctuations. Again, with chemical reaction, the turbulent mass transport could not be related to the mean transverse concentration gradient in that part of the shear layer nearer the unreacted region. The normalized cross-correlations of the streamwise- and the transverse-velocity fluctuations, however, remained negative within the entire shear layer with or without chemical reaction, indicating positive Reynolds stresses (cf. Fig. 11b).

### (B) Experiments

Experiments were continued to examine the thermal structure of premixed, rod-stabilized, lean methane/ethane/air V-flames. Errors due to the use of frequency-compensated fine-wire thermocouples were analyzed and found to lead to a possible 10 to 15% attenuation of the signals over the frequency range of interest (of less than 1000 Hz). Reasonably good agreement was also observed between our temperature measurements and the density measurements by Rayleigh scattering reported in the literature for comparable experiments, thus lending further support to the validity of our measurements.

Earlier results on the effects of the equivalence ratio and turbulence scale and intensity showed possible coupling between chemical kinetics and turbulence in the augmentation of the higher-frequency temperature fluctuations. Such coupling was also indicated in the theoretical investigation summarized above. In order to further elucidate the role of chemical kinetics, experiments were conducted to examine the effects of adding various amounts of ethane to methane/air mixtures. Figure 12 shows comparisons of the RMS temperature fluctuations within the high-frequency region at different "instantaneous" mean temperatures (pertaining to a time interval of 25 ms) for different compositions of methane/ethane/air mixtures. Again, it was noted that the presence of a 10-mesh turbulence grid led to larger RMS values than those for quasi-laminar flames (without grid-generated turbulence). The effect of ethane addition, however, was not monotonic. For both quasi-laminar and turbulent flames, the RMS values were the highest for 10%-ethane addition and became lower for 12 and 100%-ethane.

Similar difference were observed in the spectral density distributions and the probability density functions for different compositions of methane/ethane/air mixtures. Figure 13 shows comparisons of the spectral density distributions of apparent mean-square temperature fluctuations for quasi-laminar and turbulent methane/ethane/air flames. Again, the ones for 10%-ethane addition were the highest.

### (2) Major Research Equipment

In order to further understand the mechanisms governing the turbulence-combustion interactions, experiments were planned to examine simultaneous temperature and velocity fluctuations within the flame brush. A one-component Laser-Doppler-Velocimetry system (TSI 9100-6) was installed and tested. Simultaneous measurements of velocity fluctuations by means of hot-wire anemometer and LDV system were being conducted.

### (3) Genesis of Transverse Waves

A manuscript describing the genesis of transverse waves in gaseous detonations was accepted for publication in Combustion and Flame. This paper examined both numerically and analytically the stability of two-dimensional piston-supported gaseous detonations.

The numerical analysis showed many interesting results. First, in channels whose widths were smaller than or of the order of the characteristic reaction length, transverse waves did not develop and only one-dimensional longitudinal oscillations were observed. Second, a critical channel width existed beyond which a transverse wave might

develop. Third, as the channel became wider and up till a second critical channel width, the transverse wave persisted while its oscillation period became longer. Fourth, beyond that second critical channel width, new transverse waves formed, whose wavelengths were equal to the wavelength corresponding to the second critical value. Moreover, at and beyond that critical channel width, the oscillation period attained a constant value, almost identical to that of the one-dimensional oscillation. These results demonstrated the existence of a most unstable wavelength which would persist further on and govern the cell size in wide channels.

An approximate linearized stability theory previously developed for one-dimensional shock-reaction-zone complex was extended to the two-dimensional case and the mechanism of oscillation identified. It was found that the interactions between the irreversible temperature fluctuations (due to shock perturbation) and the finite reaction zone induced an oscillatory energy-source field which would generate pressure waves. The latter, in turn, perturbed the shock front and generated the temperature fluctuations, thereby completing the cycle. Stability limits as well as amplification (or attenuation) rates and oscillation periods were obtained for different transverse wave numbers at different degrees of overdrive. The amplification rates were found to decrease and become negative for larger wave numbers or for larger degrees of overdrive. In other words, transverse waves could not develop in very narrow channels or in highly overdriven detonations because of attenuation. Moreover, it was shown that for the most unstable wavelength (as observed in the numerical simulations), the oscillation period was almost equal to that of the one-dimensional oscillation.

III. Publications and Reports

See attached Enclosure.

IV. Professional Personnel

Professor T. Y. Toong and Dr. G. E. Abouseif

V. Interactions

A presentation on Turbulence-Combustion Interactions — Theory and Experiments was made by T. Y. Toong at the 1985 AFOSR/ONR Contractors Meeting on Turbulent Combustion on July 25, 1985 at the California Institute of Technology.

## THEORETICAL MODEL:

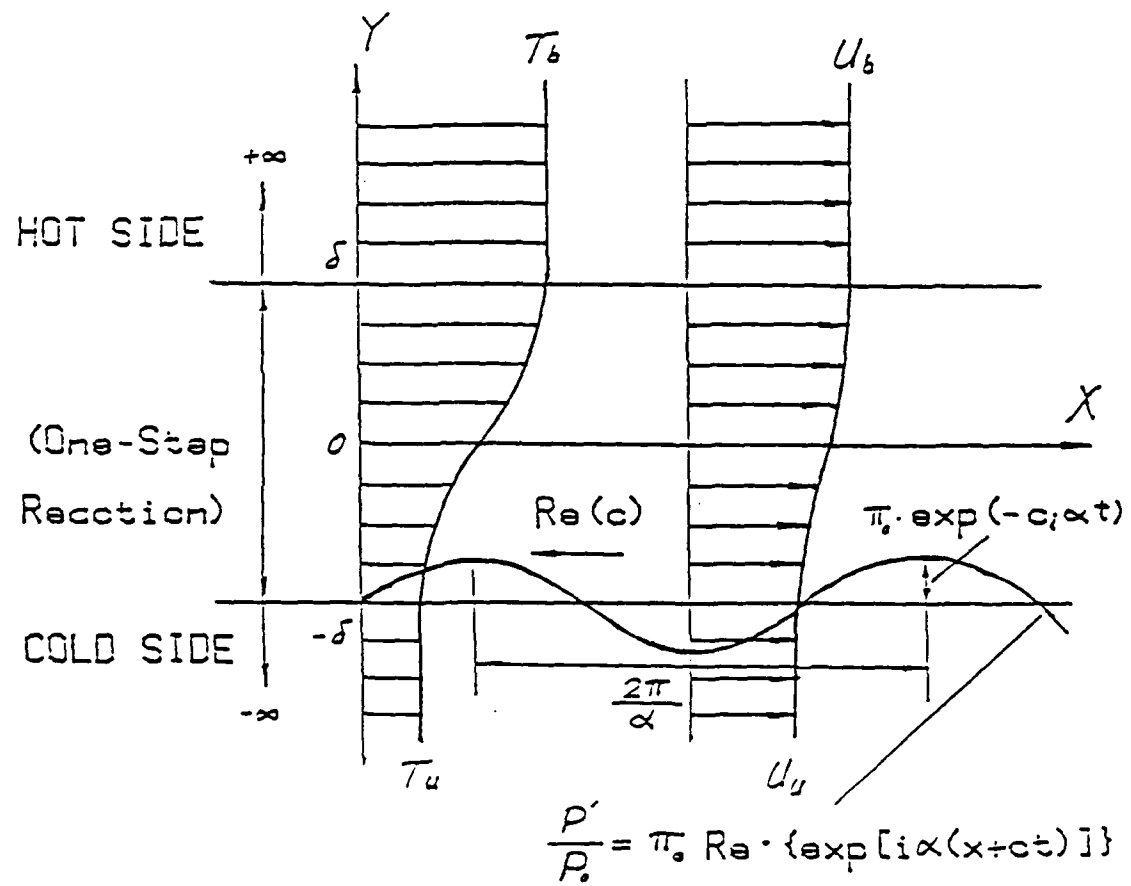
 $P_r = \text{CONSTANT EVERYWHERE}$ 

FIG. 1 MODEL

## GROWTH RATE VERSUS WAVE NUMBER:

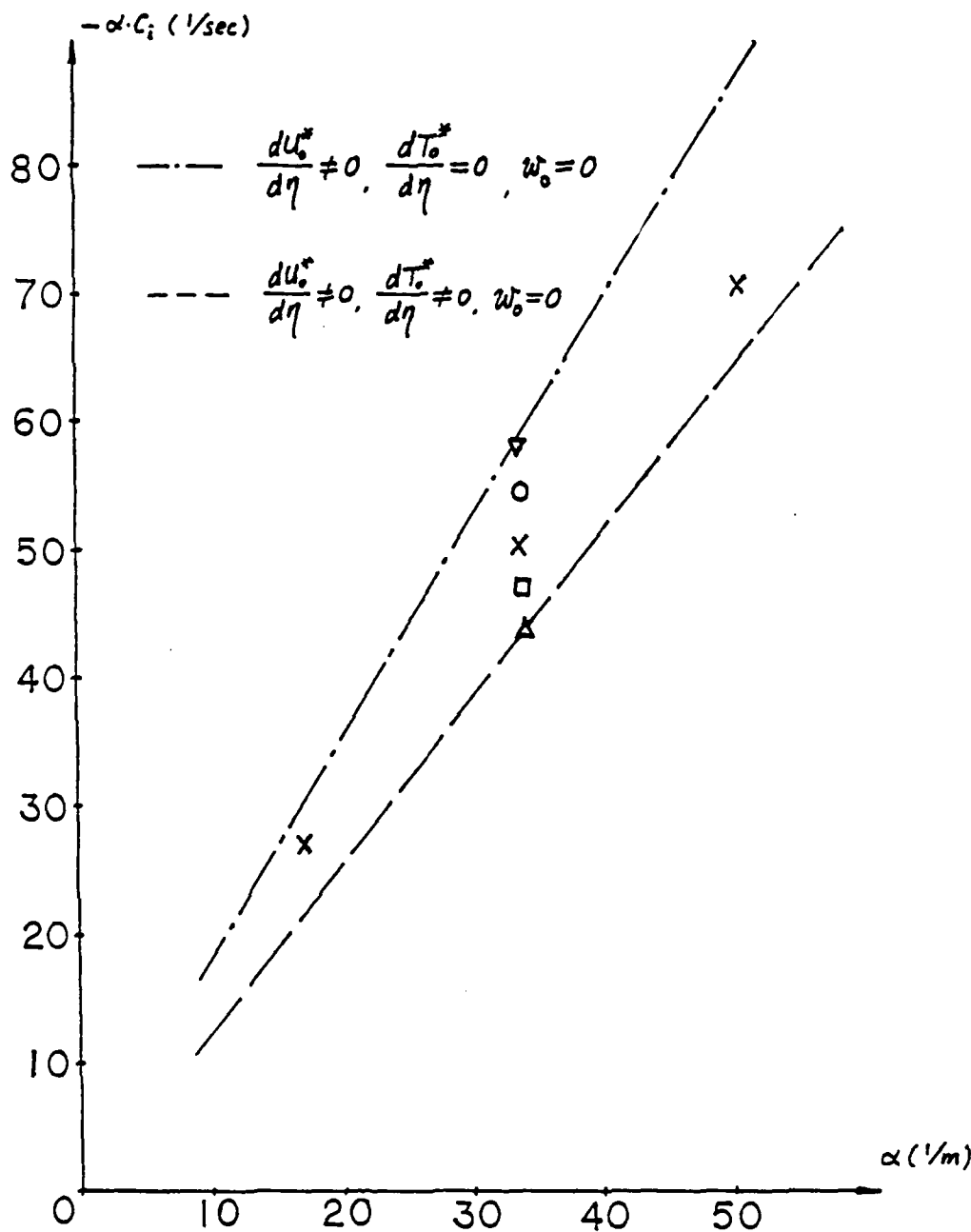


FIG. 2 EFFECTS OF CHEMICAL REACTION ON GROWTH RATE:  $\nabla, \Delta$  NON-REACTING SHEAR LAYER,  $\nabla$  WITH NO TRANSVERSE TEMPERATURE GRADIENT,  $\Delta$  WITH TRANSVERSE TEMPERATURE GRADIENT;  $O, X, \square$  REACTING SHEAR LAYER,  $O$  FASTEST REACTION RATE,  $\square$  SLOWEST REACTION RATE.

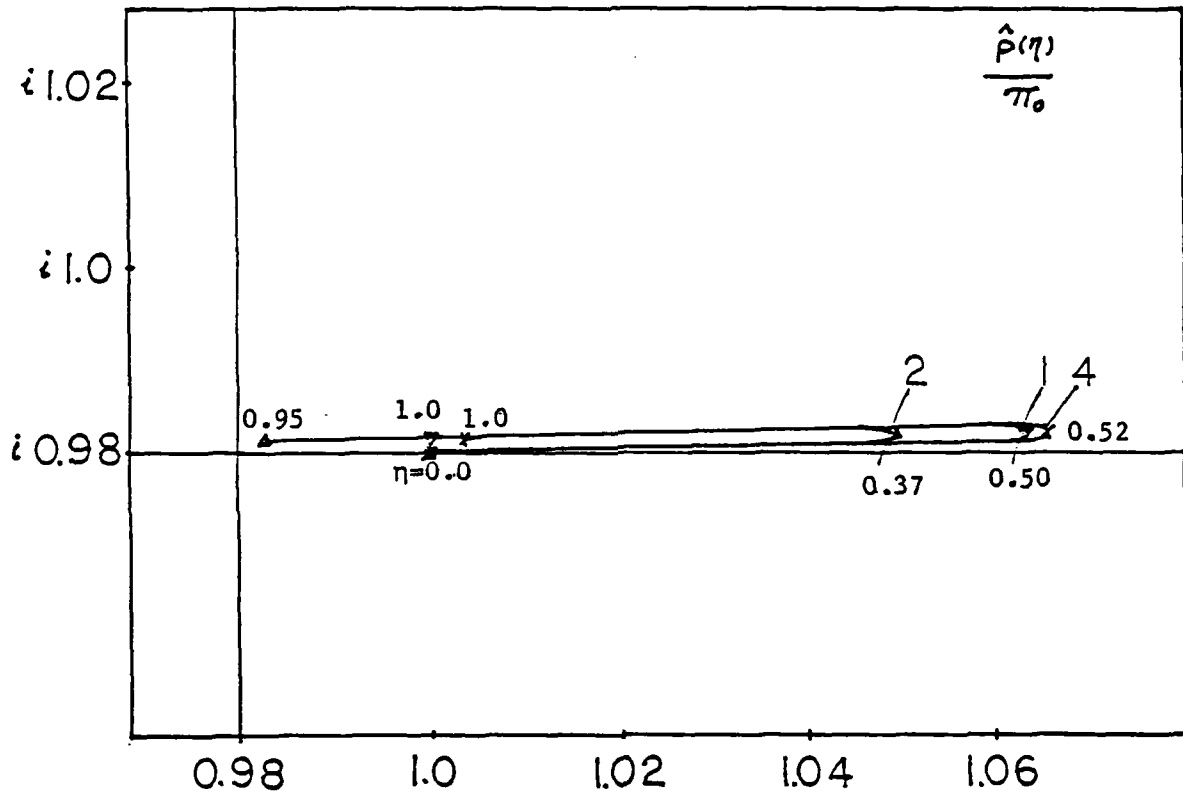
COMPLEX EIGEN-FUNCTIONS,  $\hat{p}(\eta)/\pi_0$ 

FIG. 3 COMPARISON OF PRESSURE FLUCTUATIONS IN THE PHASE PLANE AT DIFFERENT POSITIONS WITHIN THE SHEAR LAYER. CASE 1: NO REACTION, NO TRANSVERSE TEMPERATURE GRADIENT; CASE 2: NO REACTION BUT WITH TRANSVERSE TEMPERATURE GRADIENT; CASE 4: WITH REACTION AND TRANSVERSE TEMPERATURE GRADIENT.

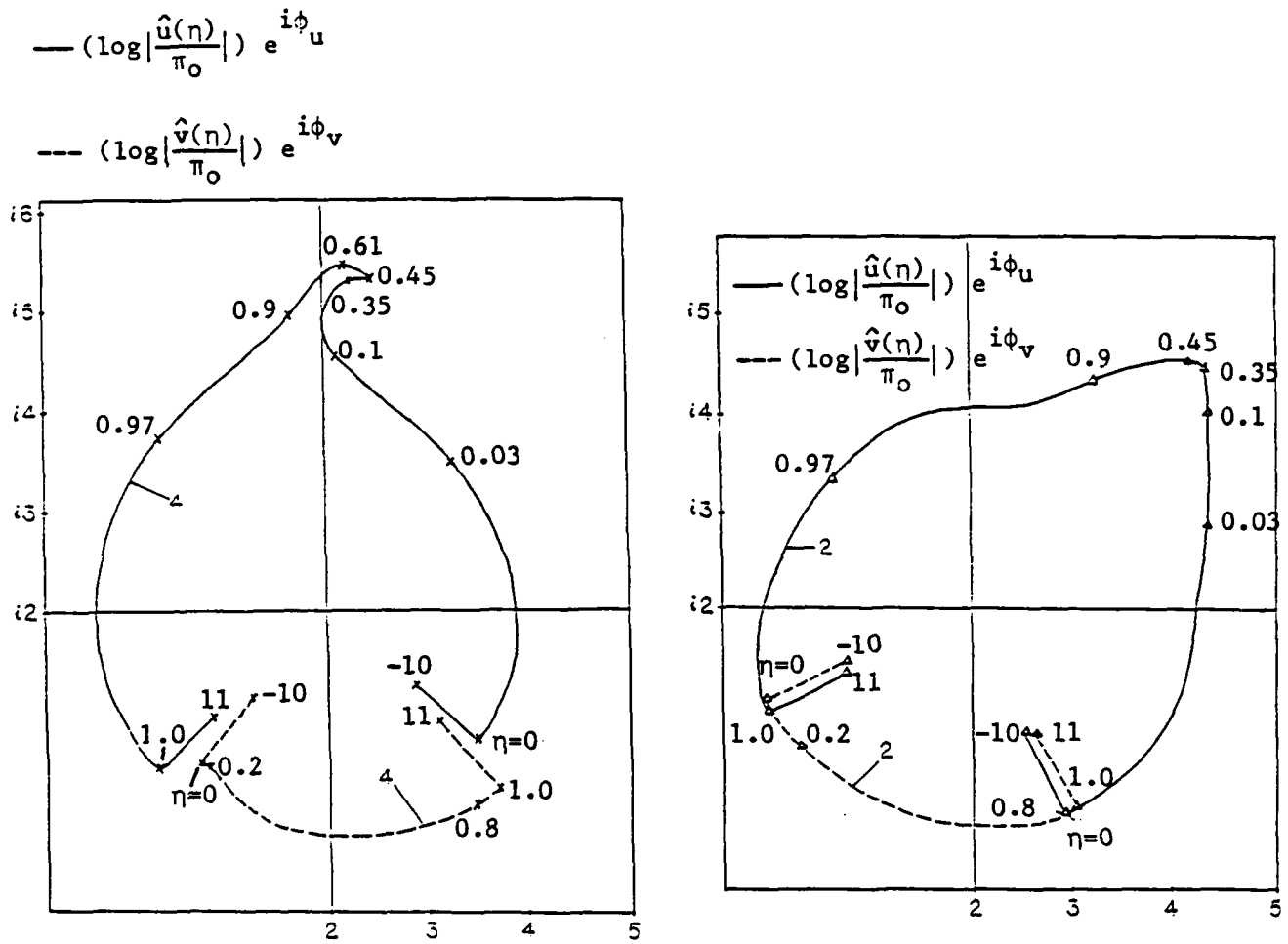
COMPLEX EIGEN-FUNCTIONS,  $\hat{u}(\eta)/\pi_0$  and  $\hat{v}(\eta)/\pi_0$ 

FIG. 4 COMPARISON OF VELOCITY FLUCTUATIONS IN THE PHASE PLANE AT DIFFERENT POSITIONS WITHIN THE SHEAR LAYER. CASE 2: NO REACTION BUT WITH TRANSVERSE TEMPERATURE GRADIENT; CASE 4: WITH REACTION AND TRANSVERSE TEMPERATURE GRADIENT. AMPLITUDES IN LOGARITHMIC SCALE.

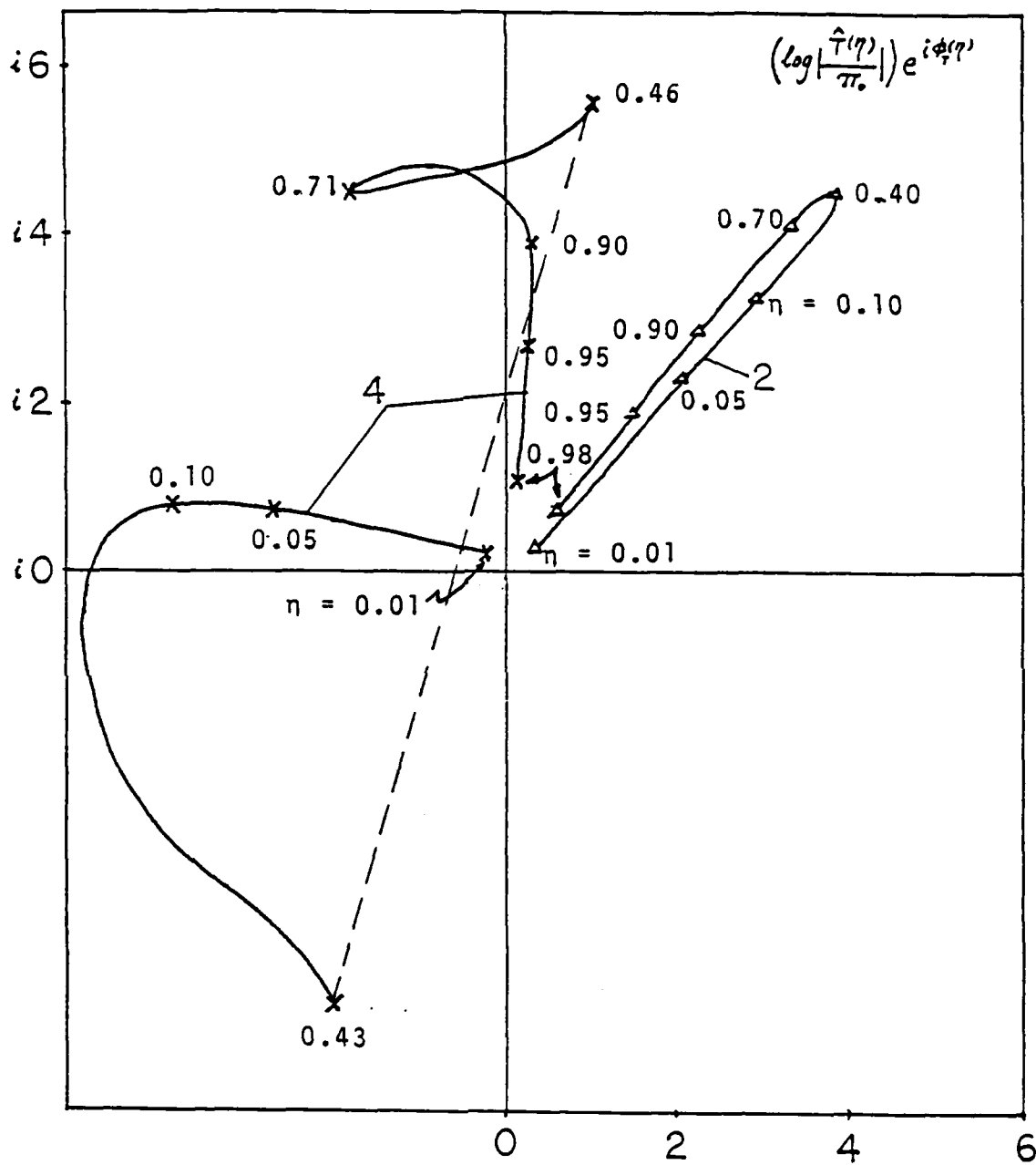


FIG. 5 COMPARISON OF TEMPERATURE FLUCTUATIONS IN THE PHASE PLANE AT DIFFERENT POSITIONS WITHIN THE SHEAR LAYER. CASE 2: NO REACTION BUT WITH TRANSVERSE TEMPERATURE GRADIENT; CASE 4: WITH REACTION AND TRANSVERSE TEMPERATURE GRADIENT. AMPLITUDES IN LOGARITHMIC SCALE.

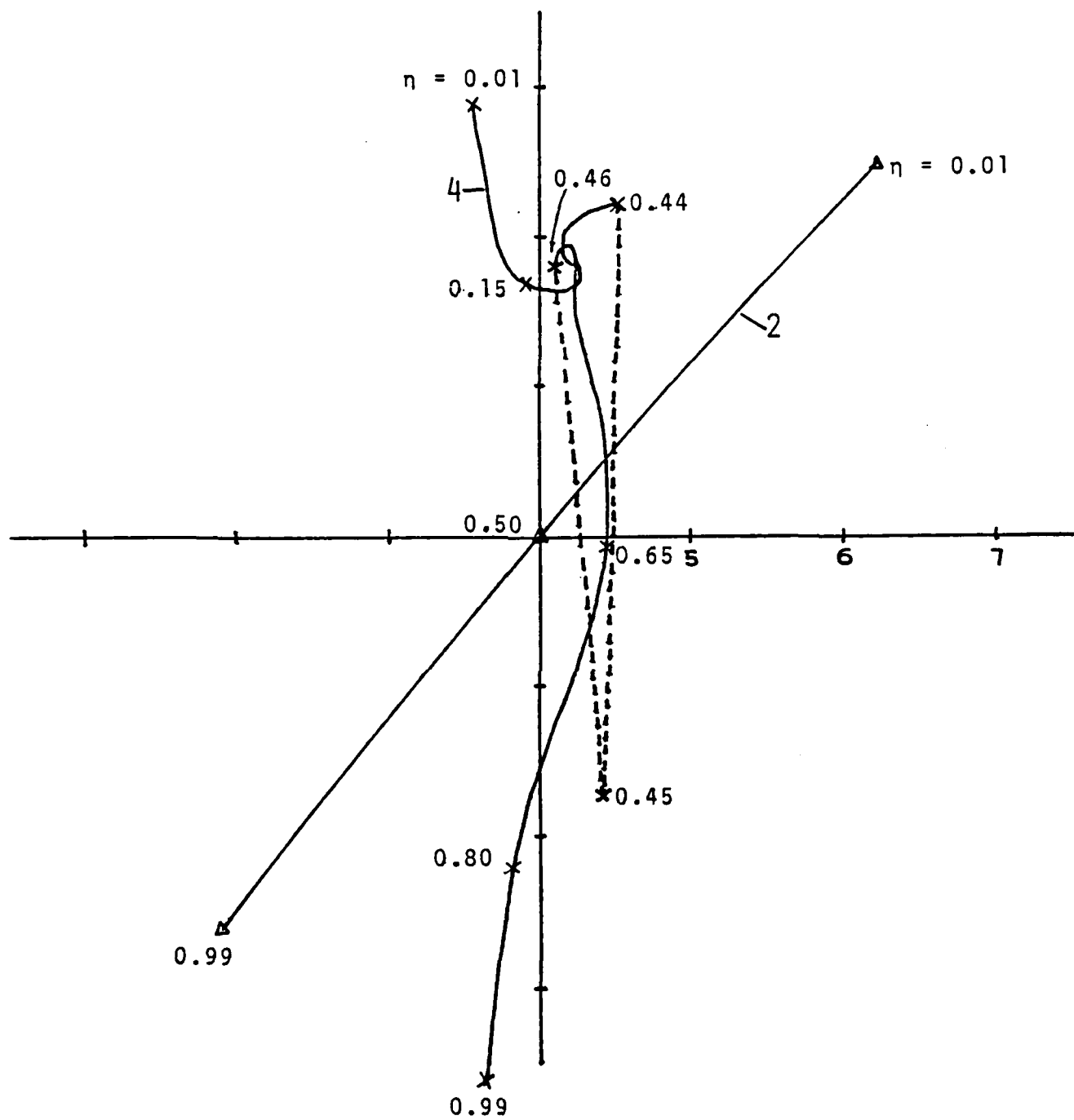


FIG. 6 COMPARISON OF VORTICITY FLUCTUATIONS IN THE PHASE PLANE AT DIFFERENT POSITIONS WITHIN THE SHEAR LAYER. CASE 2: NO REACTION BUT WITH TRANSVERSE TEMPERATURE GRADIENT; CASE 4: WITH REACTION AND TRANSVERSE TEMPERATURE GRADIENT. AMPLITUDES IN LOGARITHMIC SCALE.

PHASE RELATIONSHIPS:

19

$$\{i(c^* + u_o^*) - D_I[(\beta - m) D_{II} - m]\} \frac{\hat{T}}{\pi_o} = - \frac{u_o^*}{2\alpha\delta} \frac{1}{T_o^*} \frac{dT_o^*}{d\eta} \frac{\hat{v}}{\pi_o}$$

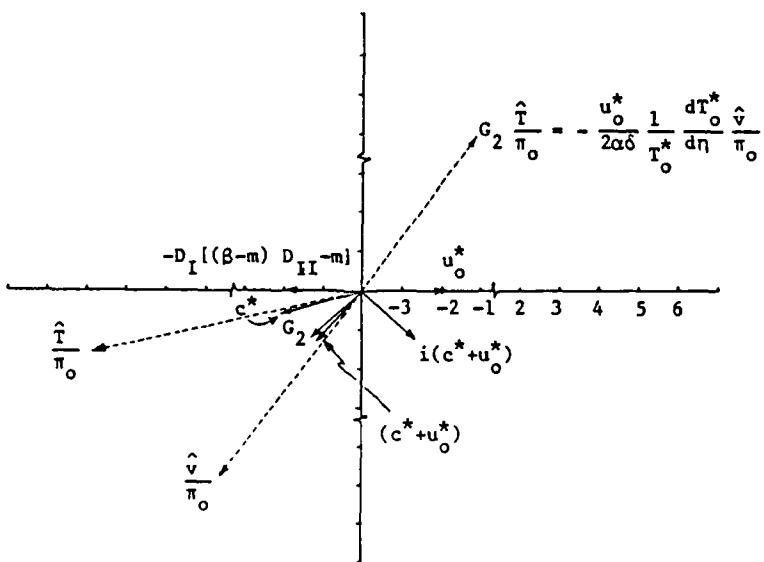
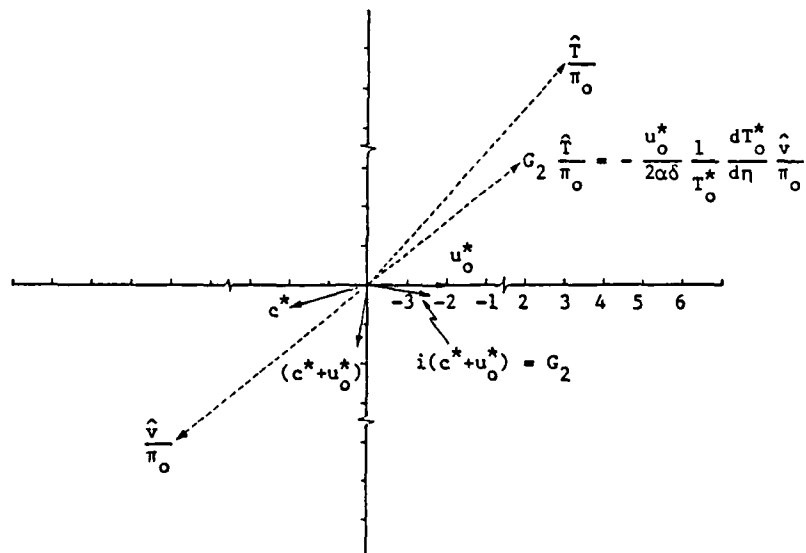


FIG. 7 PHASE RELATIONSHIPS BETWEEN TEMPERATURE AND TRANSVERSE-VELOCITY FLUCTUATIONS AT  $\eta = 0.2$ . CASE 2 (TOP): NO REACTION BUT WITH TRANSVERSE TEMPERATURE GRADIENT; CASE 4 (BOTTOM) WITH REACTION AND TRANSVERSE TEMPERATURE GRADIENT. AMPLITUDES IN LOGARITHMIC SCALE.

PHASE RELATIONSHIPS:

20

$$\{i(c^* + u_o^*) - D_I[(\beta - m) D_{II} - m]\} \frac{\hat{T}}{\pi_o} = - \frac{u_o^*}{2\alpha\delta} \frac{1}{T_o^*} \frac{dT_o^*}{d\eta} \frac{\hat{v}}{\pi_o}$$

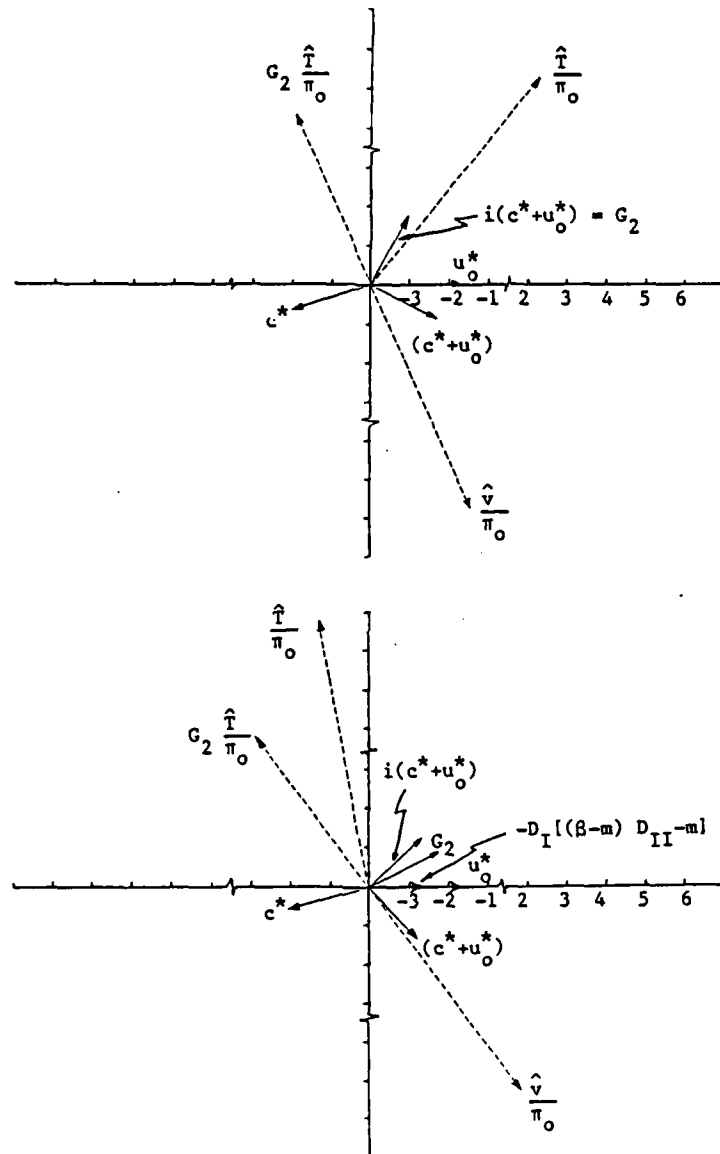


FIG. 8 PHASE RELATIONSHIPS BETWEEN TEMPERATURE AND TRANSVERSE-VELOCITY FLUCTUATIONS AT  $\eta = 0.8$ . CASE 2 (TOP): NO REACTION BUT WITH TRANSVERSE TEMPERATURE GRADIENT; CASE 4 (BOTTOM) WITH REACTION AND TRANSVERSE TEMPERATURE GRADIENT. AMPLITUDES IN LOGARITHMIC SCALE.

$$i(c^* + u_o^*) \frac{\hat{\Omega}}{\pi_o} = - \frac{u_o^*}{2\alpha\delta} \frac{d^2 u_o^*/d\eta^2}{du_o^*/d\eta} \frac{\hat{v}}{\pi_o} - D_I [(\beta-m) D_{II}^{-m}] \frac{\hat{T}}{\pi_o}$$

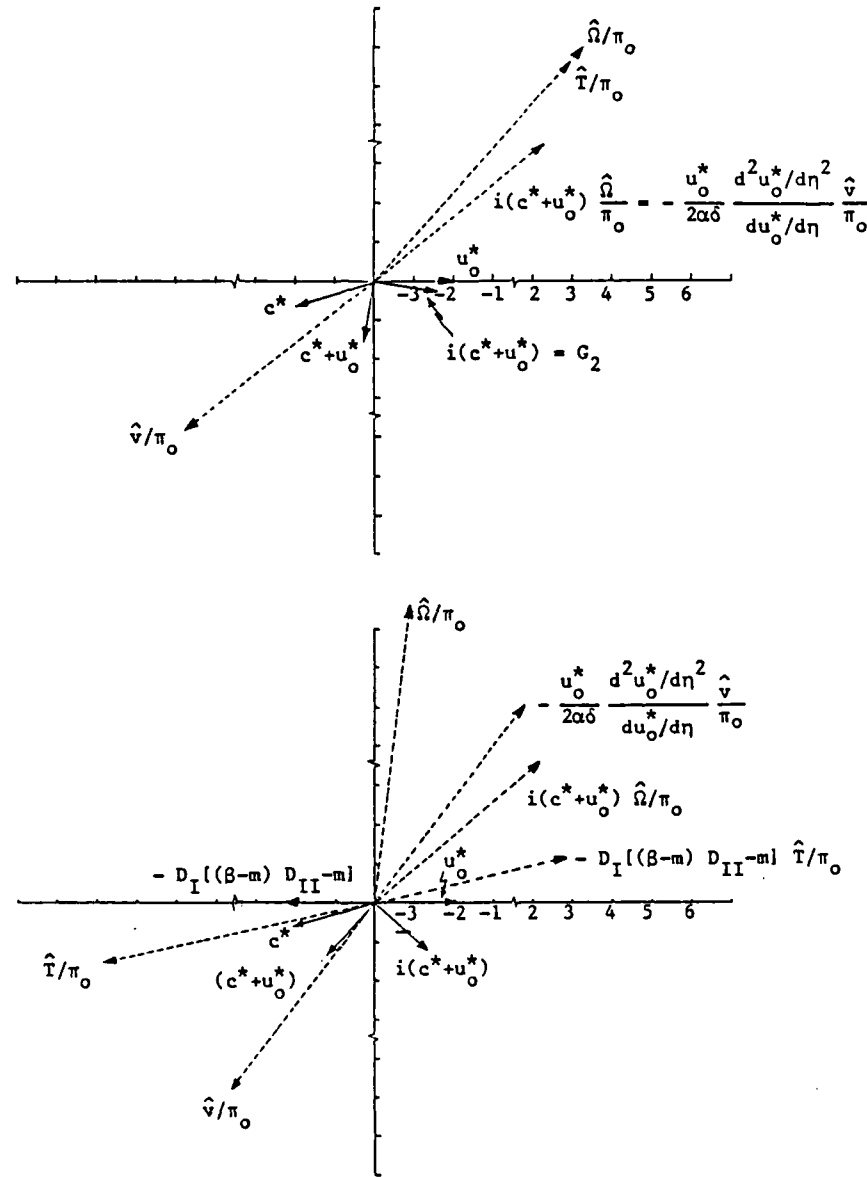


FIG. 9 PHASE RELATIONSHIPS BETWEEN VORTICITY, VELOCITY AND TEMPERATURE FLUCTUATIONS AT  $\eta = 0.2$ . CASE 2 (TOP): NO REACTION BUT WITH TRANSVERSE TEMPERATURE GRADIENT; CASE 4 (BOTTOM): WITH REACTION AND TRANSVERSE TEMPERATURE GRADIENT. AMPLITUDES IN LOGARITHMIC SCALE.

$$i(c^* + u_o^*) \frac{\hat{\Omega}}{\pi_o} = - \frac{u_o^*}{2\alpha\delta} \frac{d^2 u_o^* / d\eta^2}{du_o^* / d\eta} \frac{\hat{v}}{\pi_o} - D_I [(\beta - m) D_{II} - m] \frac{\hat{T}}{\pi_o}$$

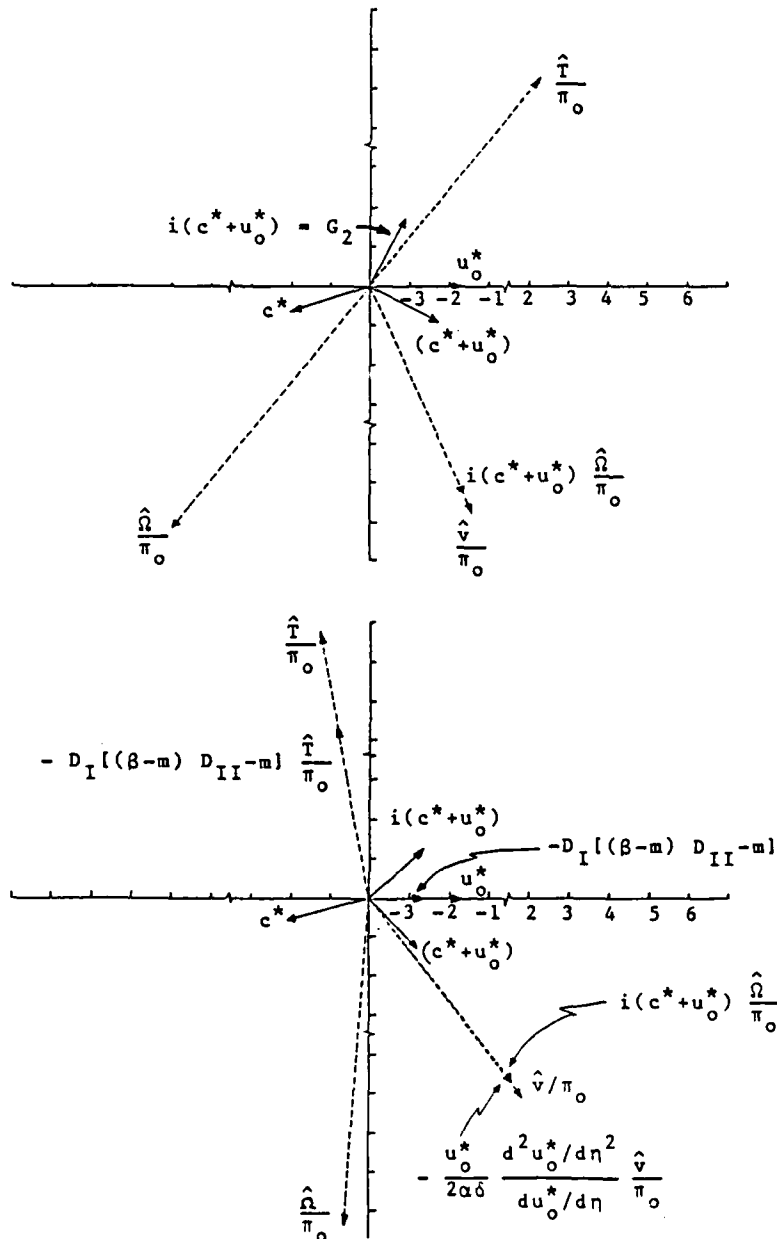
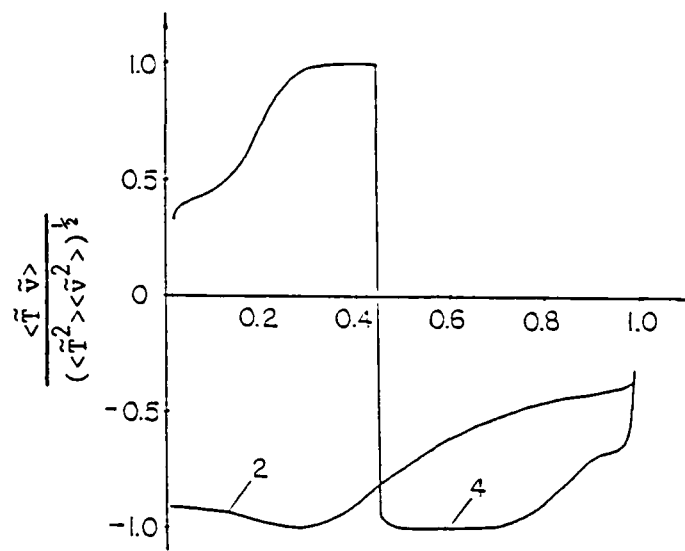
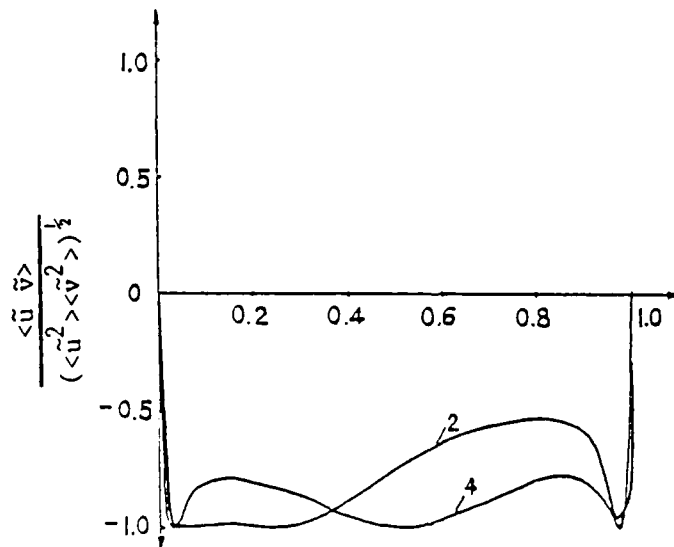


FIG. 10 PHASE RELATIONSHIPS BETWEEN VORTICITY, VELOCITY AND TEMPERATURE FLUCTUATIONS AT  $\eta = 0.8$ . CASE 2 (TOP): NO REACTION BUT WITH TRANSVERSE TEMPERATURE GRADIENT; CASE 4 (BOTTOM): WITH REACTION AND TRANSVERSE TEMPERATURE GRADIENT. AMPLITUDES IN LOGARITHMIC SCALE.



(a)



(b)

FIG. 11 (a) NORMALIZED CROSS-CORRELATIONS OF TEMPERATURE AND TRANSVERSE-VELOCITY FLUCTUATIONS (b) NORMALIZED CROSS-CORRELATIONS OF LONGITUDINAL- AND TRANSVERSE-VELOCITY FLUCTUATIONS. CASE 2: NO REACTION BUT WITH TRANSVERSE TEMPERATURE GRADIENT; CASE 4: WITH REACTION AND TRANSVERSE TEMPERATURE GRADIENT.

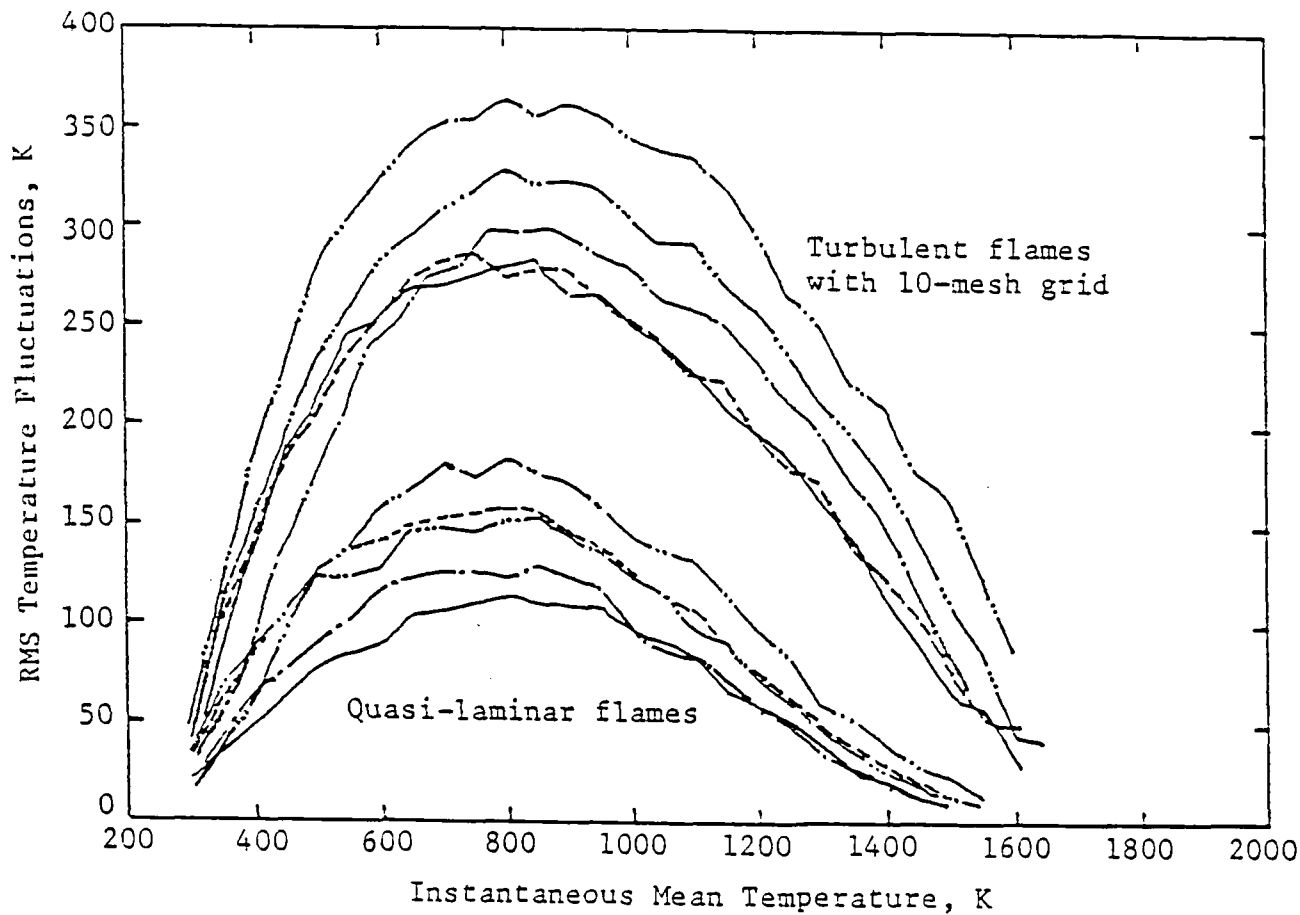


FIG. 12 COMPARISON OF RMS TEMPERATURE FLUCTUATIONS WITHIN HIGH-FREQUENCY REGION AT DIFFERENT "INSTANTANEOUS" MEAN TEMPERATURES FOR DIFFERENT COMPOSITIONS OF METHANE-ETHANE-AIR MIXTURES:  
 — 0% ETHANE, — · — 5% ETHANE, — · · — 10% ETHANE, — · · · — 12% ETHANE, ---- 100% ETHANE. TOP CURVES, WITH 10-MESH TURBULENCE GRID, BOTTOM CURVES, NO TURBULENCE GRID; EQUIVALENCE RATIO, 0.75; MEAN MIXTURE VELOCITY, 2.4 M/S; 35 MM DOWNSTREAM OF 2.1 MM-DIAMETER FLAMEHOLDER.

## EFFECTS OF ETHANE ADDITION

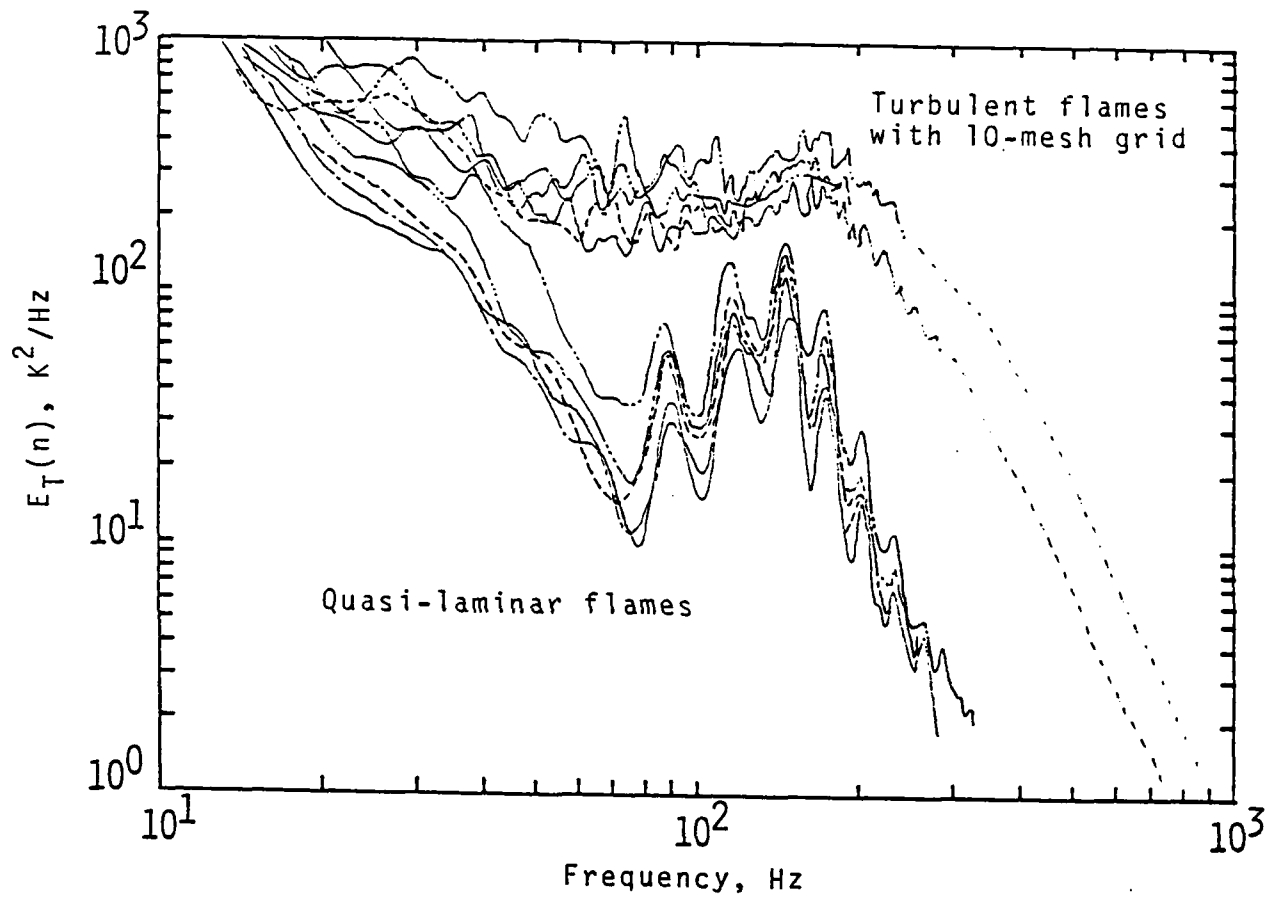
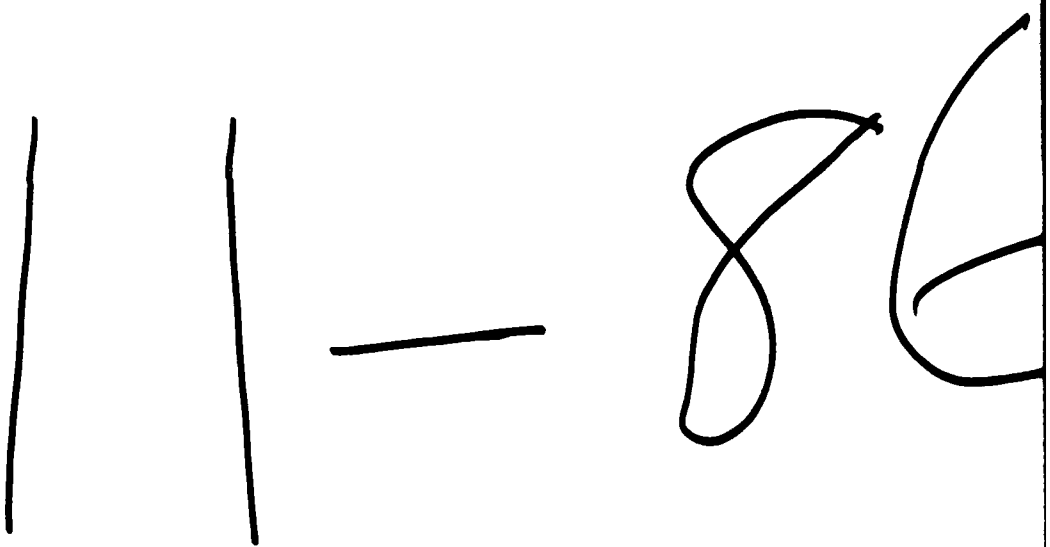
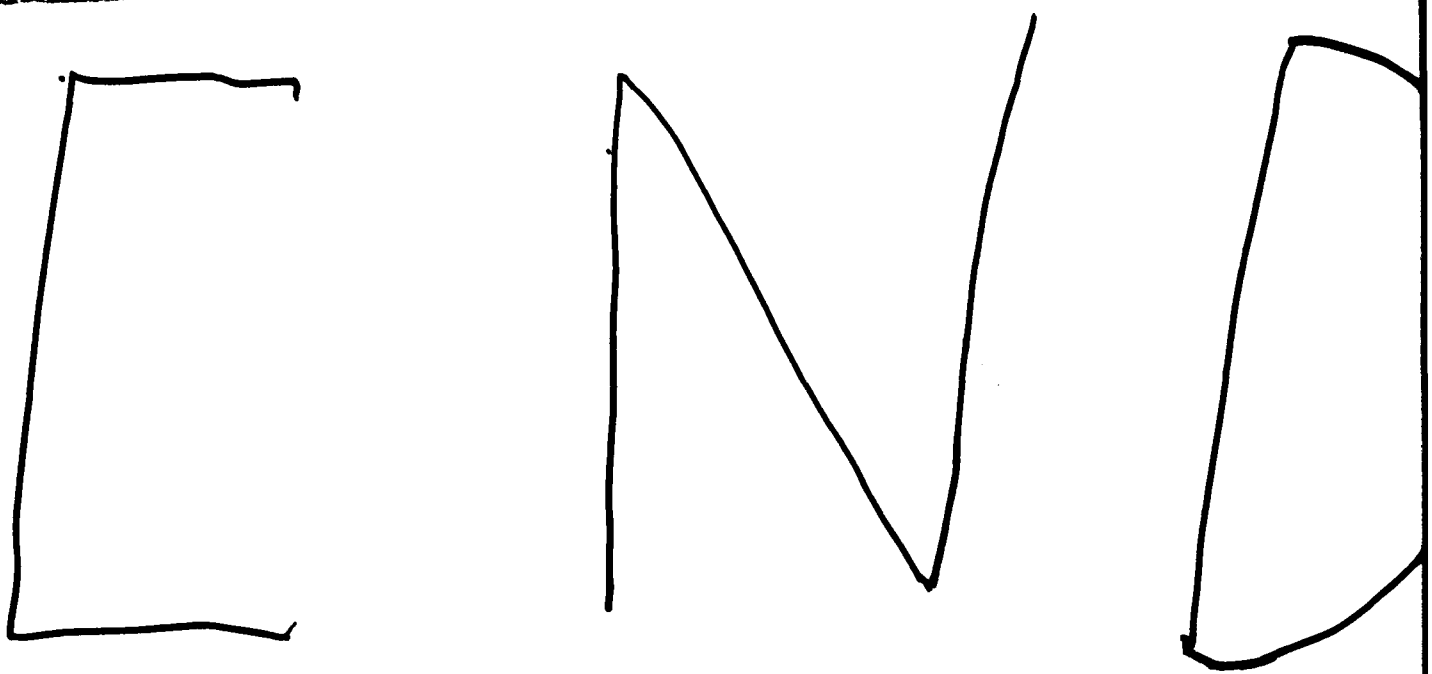


FIG. 13 COMPARISON OF SPECTRAL DENSITY DISTRIBUTIONS OF MEAN-SQUARE TEMPERATURE FLUCTUATIONS FOR DIFFERENT COMPOSITIONS OF METHANE-ETHANE-AIR MIXTURES: — 0% ETHANE, - · - 5% ETHANE, - .. - 10% ETHANE, - · · - 12% ETHANE, - - - 100% ETHANE. TOP CURVES, WITH 10-MESH TURBULENCE GRID, BOTTOM CURVES, NO TURBULENCE GRID; EQUIVALENCE RATIO, 0.75; MEAN MIXTURE VELOCITY, 2.4 M/S; MAXIMUM RMS TEMPERATURE FLUCTUATIONS AT 35 MM DOWNSTREAM OF 2.1 MM-DIAMETER FLAMEHOLDER.

## ENCLOSURE

Basic Instability Mechanisms  
in Chemically Reacting Subsonic and Supersonic Flows  
Publications and Reports  
(Grant AFOSR-83-0373)

1. Abouseif, G. E., Keklak, J. A. and Toong, T. Y., "Ramjet Rumble: The Low-Frequency Instability Mechanism in Coaxial Dump Combustors", Combustion Science and Technology, 36, pp. 83-108, 1984.
2. Abouseif, G. E. and Toong, T. Y., "Theory of Unstable Two-Dimensional Detonations: Genesis of Transverse Waves", Combustion and Flame, in press.
3. Toong, T. Y., "Turbulence-Combustion Interactions", in preparation.



D T / C